TEXT

Introduction

Precise identification and preservation of the pyramidal tract during surgery for parenchymal brain tumors is of crucial importance for avoidance of postoperative deterioration of the motor function. Intraoperative subcortical brain mapping with electrical stimulation [1,2], as well as neuronavigation, based on preoperative diffusion-weighted imaging (DWI) or diffusion tensor imaging (DTI) [3-10], are usually used for this purpose, but both of these techniques has a recognizable pitfalls. The first one can provide only functional information and does not permit precise estimation of the exact course of the pyramidal tract, whereas the second is susceptible to mislocalization errors, particularly caused by brain shift [11,12]. Technique of intraoperative DWI (iDWI) using intraoperative MR scanner of low magnetic field strength (0.3 Tesla), has been developed recently in Tokyo Women`s Medical University [13,14]. After validation of the scanning protocol during pre-clinical investigation on volunteers [15], the clinical part of the study was initiated with an objective to evaluate the usefulness and efficacy of iDWI during surgical management of gliomas.

Methods and Materials

Main principles of surgery for gliomas with use of iMRI of low (0.3 Tesla) magnetic field strength (AIRIS II, Hitachi Medical, Tokyo, Japan) adopted in the Tokyo Women`s Medical University had been presented previously [16]. Shortly, after induction of the general anesthesia, the patient head was firmly fixed with titanium pins in the modified Sugita head-holder (Fig.1), representing lower arch of the headholder-coil (Mizuho Ltd., Tokyo, Japan). The head-holder was connected to the operating table with supporting arm incorporating 3 joints and 2 rotational axes, which provided easy adjustment of the head position according to the surgical needs. For preservation of sterile conditions in the surgical field during the procedure the patient head was covered with transparent drapes, whereas electrical connectors of the headholder-coil were protected with special caps to prevent contamination with fluids and dust. Before start of iMRI several fiducial markers were fixed to the skull on the periphery of the surgical field, and additional one was inserted into the surgical wound and located in the vicinity to the target. The protective caps were removed from the electrical connectors and both semicircular

arches of the headholder-coil were connected. Wide transparent sterile drape was used to cover the whole body of the patient, his or her head, and surgical wound, and the operating table was moved into gap of the intraoperative MR scanner. During routine surgery iMRI was usually performed at least 2 times: after craniotomy and completeness of the approach to the tumor and after resection of the neoplasm. If additional resection of glioma was required iMRI investigation was repeated.

Clinical data

Evaluation of the clinical usefulness of iDWI was performed in 10 surgically treated patients with gliomas located in the vicinity to the pyramidal tract. There were 5 men and 5 women with a mean age of 41.2 ± 13.9 years (range: 26 – 68 years). Initially diagnosed tumors were met in 8 patients, whereas recurrent in 2. According to histopathological examination there were two astrocytomas WHO grade II, two anaplastic astrocytomas WHO grade III, two anaplastic oligodendrogliomas WHO grade III, and four glioblastomas WHO grade IV. Nine patients were operated on in supine, and one in prone position. The study was approved by responsible authorities of the Tokyo Women`s Medical University and informed consent was obtained from each patient and his/her nearest family member.

Evaluation of the pyramidal tract contrasting

According to objectives of the present study in all cases in addition to usually used axial T_2-weighted and axial T_1-weighted imaging with or without contrast enhancement, which took approximately 10 minutes, additional shimming, DWI, and coronal T_1-weighted imaging were done, which required additional 15 – 20 minutes. T_1-weighted images and T_2-weighted images were obtained using, respectively, 3D gradient echo (RSSG, RF-spoiled steady state acquisition rewound gradient echo with TR 27 ms and TE 10ms), and 3D fast spin echo with driven equilibrium pulse (TR 1000 ms, TE 140 ms), with scan matrix size 256 × 160, 100 slices, 1.5 mm slice interval for both imagings. DWI was acquired according to the protocol described previously [15] using application of the motion probing gradient (MPG) pulse in anteroposterior direction taken into account the actual position of the patient head. iDWI was performed both before and after tumor resection in 9 cases, and only

before tumor removal in one. Two evaluations (one before and one after tumor resection) were excluded from the further analysis due to violation of the unified protocol for iDWI. Seventeen residual investigations, incorporating 306 slices, were evaluated, and pyramidal tract contrast ratios were measured as described previously [15], and compared between affected and non-affected sides. Additionally, the contrast ratio of pyramidal tracts was compared between patients and previously investigated healthy volunteers [15].

Evaluation of iDWI accuracy

For evaluation of distortion artifacts on iDWI the distances between image centerline (near the midline) to the lateral cerebral ventricle wall, indicating the position of the pyramidal tract, and to the cortical surface were measured, correspondingly in 11 affected and 15 non-affected sides (with the exception of cases in which lateral ventricle wall could not be identified due to mass effect), and 17 affected and 17 non-affected sides. The same distances were measured on T_1-weighted images. The differences of these measurements were calculated and named as distortion indices corresponding to displacement of the lateral ventricle and displacement of the cortical surface, which were compared between each other.

Evaluation of the clinical usefulness of iDWI

For evaluation of the clinical utility of iDWI during surgery for gliomas, 5 neurosurgeons with an average surgical experience of 12.6 ± 4.7 years (range: 8 – 20 years) were asked to complete a specially designed questionnaire and to answer whether iDWI-based determination of the pyramidal tract was useful and for which purpose, and what problems of this technique are seemingly interfere with the clinical needs.

Statistics

Two-tailed t-test was used for statistical analysis. The level of significance was determined at $P < 0.05$.

Results

Using of the modified Sugita head-holder (lower arch of the headholder-coil) during microneurosurgical

procedure provided firm and stable fixation of the patient head and was not accompanied by any troubles in any case. In all 10 patients intraoperative T_1-weighted and T_2-weighted images provided sufficient visualization of the brain tumor, as well as its remnants after incomplete resection (Fig.2). The total iMRI investigation time in cases which included iDWI, calculated from attachment of the upper semicircular arch of the headholder-coil to its removal for continuation of the surgical procedure, constituted approximately 40 minutes.

Evaluation of the pyramidal tract contrasting

iDWI permitted visualization of the pyramidal tract on the non-affected side in all 10 cases, and on the affected side in 8 cases (Fig.3). In 2 patients with malignant gliomas clear visualization of the pyramidal tract on the affected side was not possible (Fig.4). The tract contrast ratios varied from 84.5% to 17.7%, and constituted in average 43.7±16.4%. The differences of the tract contrast ratio between non-affected and affected side, as well as between patients and previously investigated healthy volunteers [15] were not statistically significant. Motion artifacts were observed in four patients with pulse rate over 70 per minute, but were not an obstacle for identification of the pyramidal tract position by neurosurgeons.

Evaluation of iDWI accuracy

The average displacement at the lateral ventricle on the affected side constituted 1.0±0.7 mm. The differences of the distortion indices between lateral ventricle wall and cortical surface were not statistically significant on the affected side, but were significant on non-affected one (Table 1). Good correspondence of the anatomical landmarks localization on iDWI and T_1-weighted imaging was found (Fig.5).

Evaluation of the clinical usefulness of iDWI

All participating neurosurgeons agreed, that iDWI was very useful for localization of the pyramidal tract and for clarification of its spatial relationships with glial tumors and normal cerebral tissue in the majority of patients (Table 2). Among problems, which can interfere with the clinical needs, increase of required iMRI examination time, and poor tract visualization in some cases of malignant gliomas, were marked.

Discussion

Simultaneous use of iDWI and structural iMRI during surgery for parenchymal brain tumors seems to be extremely useful for determination of both white matter tracts position and lesion location. However, additional incorporation of iDWI into intraoperative neuronavigation system requires high level of image quality and positional accuracy. We estimated that the latter should be within 5 mm, which corresponds to the conducting depth of the electrical stimulation during subcortical brain mapping. It was previously shown, that mean error of the intraoperative neuronavigation system using T_1-weighted images obtained with MR scanner of low magnetic field strength (0.3 Tesla) in the "intelligent operating theater" of the Tokyo Women`s Medical University is as low as 0.90 ± 0.35 mm [17]. In the present study the misalignments between DWI and T_1-weighted images on the affected side were 1.0 ± 0.7 mm for the lateral ventricle wall and 1.2 ± 1.1 mm for the cortical surface, which corresponds to the estimated positional accuracy of approximately 2.1 mm, and, in our opinion, fulfils clinical needs.

Motion artifacts were observed in four patients with pulse rate over 70 per minute. Jiang et al. [18] reported, that effect of pulsation can be minimized by avoiding the period of 100 to 250 msec after systole for data acquisition. In our pre-clinical study [15] motion artifacts in multi-shot DWI-echo-planar imaging were successfully suppressed by setting time delay from the systole on more than 300 msec. It should be marked, that under general anesthesia, pulse rate is usually well controlled. Nevertheless, in no one case motion artifacts interfered with identification of the pyramidal tract position by neurosurgeons.

Diffusion anisotropy of the white matter tracts may be reduced by presence of the lesion or perilesional edema [19]. In some cases of the present study location of malignant glioma in the close proximity to the pyramidal tract resulted in its poor visualization on iDWI. While pre-operative DWI can define whether pyramidal tract can be visualized or not, it may not correspond completely to results of intraoperative imaging. Using of visual comparison of images obtained with different directions of MPG pulses, Krings et al. [6] were able to differentiate

edema from the large descending fiber tracts in all 10 patients with various brain lesions.

All neurosurgeons participating in the present study found iDWI very useful for determination of the pyramidal tract positioning and its spatial relationships with the lesion and surgical instruments. It may become even more convenient in the future, due to development of the special sound alarm, which will be automatically activated when surgical manipulations would come into close proximity to the pyramidal tract [20]. It should be marked, however, that protocol used for acquisition of iDWI provided limited image resolution of 2.5 × 2.7 mm in both mediolateral and craniocaudal directions, whereas slice thickness of 8 mm resulted in partial volume effect. These factors can reduce differentiation of the fine structures within the pyramidal tract, and necessitate use of subcortical brain mapping with electrical stimulation in addition to iDWI [9,21].

Prolongation of time required for examination, which constituted approximately 40 minutes, was marked as a problem, which can interfere with the clinical usefulness of the technique. In fact, investigation time can be shorten if coronal T_1-weighted would be omitted and shimming would be minimized to the region-of-interest. From another side, similarly to any other type of iMRI potential decrease of postoperative morbidity and improvement of quality of life can be considered as a reasonable prize for prolongation of the total length of surgery.

In conclusion, the results of the present clinical study show, that iDWI using MR scanner of low magnetic field strength (0.3 Tesla) in the majority of patients permits clear visualization of the pyramidal tract and identification of its spatial relationships with the lesion and surgical instruments. Image quality and accuracy were sufficient for possible incorporation of iDWI into intraoperative neuronavigation system. Using of iDWI in addition to structural iMRI and subcortical functional mapping with electrical stimulation can potentially result in reduction of the postoperative morbidity after aggressive surgical removal of lesions located in the vicinity to the motor white matter tracts.

Acknowledgements

The authors are thankful to Drs. Tomokatsu Hori, Mikhail Chernov, Kyojiro Nambu and Yuji Okawara (Tokyo Women`s Medical University) and Dr. Thomas Georg Gasser (University of Duisburg-Essen) for invaluable advices and help with preparation of the manuscript. This work was supported by the Program for Promoting the Establishment of Strategic Research Centers, Special Coordination Funds for Promoting Science and Technology, Ministry of Education, Culture, Sports, Science and Technology (Japan). The presented study was supported by the Industrial Technology Research Grant Program in 2000-2005 (A45003a) from the New Energy and Industrial Technology Development Organization of Japan to Yoshihiro Muragaki.

Table 1. Comparison of distortion indices calculated using intraoperative DWI and T_1-weighted images obtained with MR scanner of low magnetic field strength (0.3 Tesla).

	Affected side	Non-affected side
Displacement of the lateral ventricle (mm)	1.0 ± 0.7 (n = 11)	0.6 ± 0.5 (n = 15)
Displacement of the cortical surface (mm)	1.2 ± 1.1 (n = 17)	0.9 ± 0.5 (n = 17)
P-value	NS	< 0.05

Data presented as mean ± standard deviation; NS: non-significant; n: number of cases

Table 2 Results of the evaluation of usefulness of intraoperative DWI for visualization of the pyramidal tract

Standard questions to five practicing neurosurgeons	Number of answers
Whether visualization of the pyramidal tract with iDWI was:	
very useful	5 (100%)
useful	0
not useful	0
Whether visualization of the pyramidal tract with iDWI was useful for:	
determination of its position	5 (100%)
determination of its shift	2 (40%)
determination of its spatial interrelationships with the lesion	5 (100%)
for other purposes	0
What problems with iDWI were encountered:	
long imaging time	5 (100%)
poor contrasting of the pyramidal tract	1 (20%)
poor image resolution	0
low signal-to-noise ratio	0
presence of image artifacts	0
others	3 (60%)

iDWI: intraoperative diffusion-weighted imaging

References

1. Woolsey CN, Erickson TC, Gilson WE. Localization in somatic sensory and motor areas of human cerebral cortex as determined by direct recording of evoked potentials and electrical stimulation. J Neurosurg 1979; 51: 476 – 506
2. Yingling CD, Ojemann S, Dodson B, Harrington MJ, Berger MS. Identification of motor pathways during tumor surgery facilitated by multichannel electromyographic recording. J Neurosurg 1999; 91: 922 – 927
3. Stejskal EO, Tanner JE. Spin diffusion measurements: spin-echoes in the presence of a time-dependent field gradient. J Chem Phys 1965; 42: 288 – 292
4. Le Bihan D, Breton E, Lallemand D, Grenier P, Cabanis E, Laval-Jeantet M. MR imaging of intravoxel incoherent motions: application to diffusion and perfusion in neurologic disorders. Radiology 1986; 161: 401 – 407
5. Pajevic S, Pierpaoli C. Color schemes to represent the orientation of anisotropic tissues from diffusion tensor data: application to white matter fiber tract mapping in the human brain. Magn Reson Med 1999; 42: 526 – 540
6. Krings T, Reinges MHT, Thiex R, Gilsbach JM, Thron A. Functional and diffusion-weighted magnetic resonance images of space-occupying lesions affecting the motor system: imaging the motor cortex and pyramidal tracts. J Neurosurg 2001; 95: 816 – 824
7. Kamada K, Houkin K, Iwasaki Y, Takeuchi F, Kuriki S, Mitsumori K, Sawamura Y. Rapid identification of the primary motor area by using magnetic resonance axonography. J Neurosurg 2002; 97: 558 – 567
8. Coenen VA, Krings T, Axer H, Weidemann J, Kranzlein H, Hans FJ, Thron A, Gilsbach JM, Rohde V. Intraoperative three-dimensional visualization of the pyramidal tract in a neuronavigation system (PTV) reliably predicts true position of principal motor pathways. Surg Neurol 2003; 60: 381 – 390
9. Berman JI, Berger MS, Mukherjee P, Henry RG. Diffusion-tensor imaging-guided tracking of fibers of the pyramidal tract combined with intraoperative cortical stimulation mapping in patients with gliomas. J

Neurosurg 2004; 101: 66 – 72

10. Kinoshita M, Yamada K, Hashimoto N, Kato A, Izumoto S, Baba T, Maruno M, Nishimura T, Yoshimine T. Fiber-tracking does not accurately estimate size of fiber bundle in pathological condition: initial neurosurgical experience using neuronavigation and subcortical white matter stimulation. Neuroimage 2005; 25: 424 – 429
11. Dorward NL, Alberti O, Velani B, Gerritsen FA, Harkness WF, Kitchen ND, Thomas DG. Postimaging brain distortion: Magnitude, correlates, and impact on neuronavigation. J Neurosurg 1998; 88: 656 – 662
12. Nabavi A, Black PM, Gering DT, Westin CF, Mehta V, Pergolizzi RS Jr, Ferrant M, Warfield SK, Hata N, Schwartz RB, Wells WM III, Kikinis R, Jolesz FA. Serial intraoperative magnetic resonance imaging of brain shift. Neurosurgery 2001; 48: 787 – 798
13. Ozawa N, Muragaki Y, Shirakawa H, Suzukawa K, Nakamura R, Watanabe S, Iseki H, Takakura K. Development of navigation system employing intraoperative diffusion weighted imaging using open MRI. In: Lemke HU, Vannier MW, Inamura K, Farman AG, Doi K, Reiber JHC (eds). Computer assisted radiology and surgery: Proceedings of the 18th International Congress and Exhibition. Amsterdam: Elseiver, 2004: 697 – 702
14. Ozawa N, Muragaki Y, Shirakawa H, Suzukawa H, Nakamura R, Iseki H. Navigation system based on intraoperative diffusion weighted imaging using open MRI. In: Lemke HU, Inamura K, Doi K, Vannier MW, Farman AG (eds). Computer assisted radiology and surgery: Proceedings of the 19th International Congress and Exhibition. Amsterdam: Elseiver, 2005: 810 – 814
15. Ozawa N, Muragaki Y, Nakamura R, Iseki H. Intraoperative diffusion-weighted imaging for visualization of the pyramidal tracts. Part I: pre-clinical validation of the scanning protocol. Minim Invasive Neurosurg 2007 (in press)
16. Muragaki Y, Iseki H, Maruyama T, Kawamata T, Yamane F, Nakamura R, Kubo O, Takakura K, Hori T. Usefulness of intraoperative magnetic resonance imaging for glioma surgery. Acta Neurochir Suppl 2006; 98: 67 – 75
17. Sugiura M, Muragaki Y, Nakamura R, Hori T, Iseki H. [Accuracy evaluation of an update-navigation system for the resection surgery of brain tumor using intraoperative magnetic resonance imaging.] J JSCAS 2005; 7:

43 – 49 (article in Japanese)

18. Jiang H, Golay X, van Zijl PC, Mori S. Origin and minimization of residual motion-related artifacts in navigator-corrected segmented diffusion-weighted EPI of the human brain. Magn Reson Med 2002; 47: 818 – 822

19. Field AS, Alexander AL, Wu YC, Hasan KM, Witwer B, Badie B. Diffusion tensor eigenvector directional color imaging patterns in the evaluation of cerebral white matter tracts altered by tumor. J Magn Reson Imaging 2004; 20: 555 – 562

20. Ozawa N, Muragaki Y, Suzukawa H, Nakamura R. Iseki H. Pyramidal tract navigation based on intraoperative diffusion-weighted imaging; sound navigation using the fiber tract margin (abstract). Int J Comput Assist Radiol Surg 2006; 1(Suppl.1): 488

21. Ozawa N, Muragaki Y, Shirakawa H, Suzukawa H, Nakamura R, Iseki H. Pyramidal tract navigation based on diffusion weighted imaging updated by intraoperative open MRI (abstract). In: Proceedings of the 13th Annual Meeting of ISMRM, Miami, 2005: abstract 2155

LEGENDS FOR FIGURES

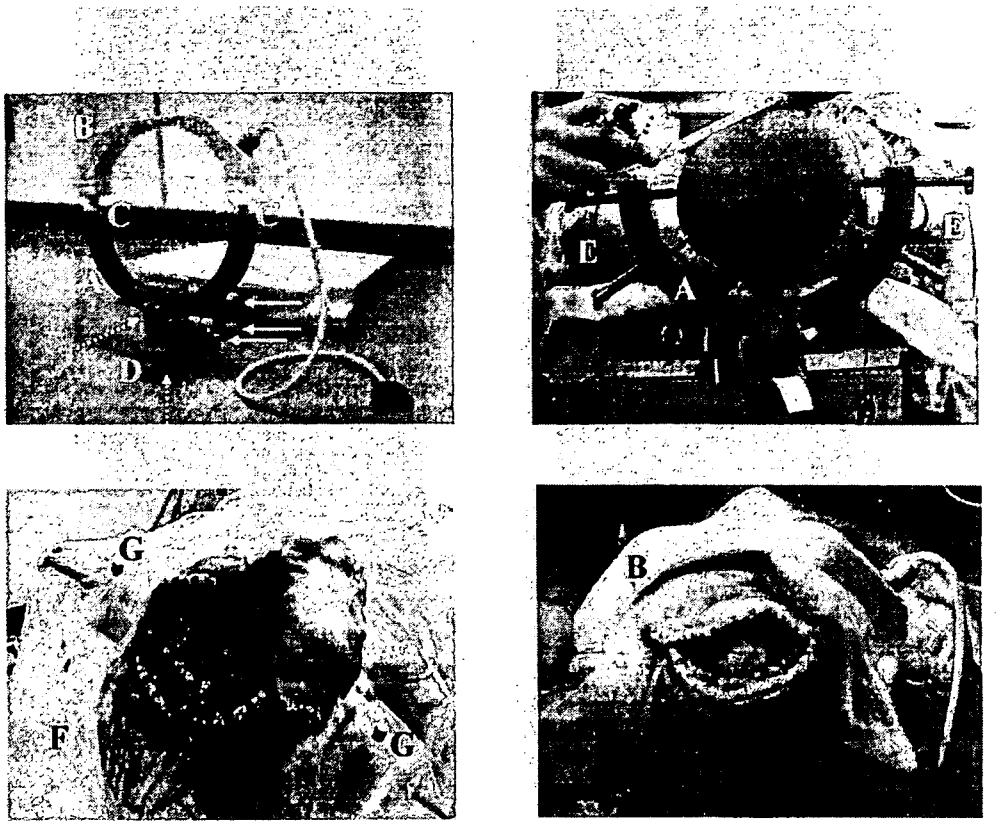

Figure 1

Radiofrequency receiver coil integrated with modified Sugita head holder for intraoperative MRI (Headholder-coil; Mizuho Ltd., Tokyo, Japan): general view of the device (*upper left*), fixation of the patient head within modified Sugita head holder before craniotomy (*upper right*) and during the surgical procedure (*lower left*), connection of both semicircular arches before intraoperative imaging, which provides solenoid coil structure (*lower right*). Marked: modified Sugita head holder with built-in cupper wire (A), removable upper semicircular arch (B), electrical connectors (C), supporting arm for fixation to the operating table (D) with its 3 joints (solid arrows) and 2 rotational axes (dashed arrows) for adjustment of the patient head position; titanium fixation pins (E), sterile surgical drapes (F), sterile protective caps, covering the electrical connectors during surgery (G).

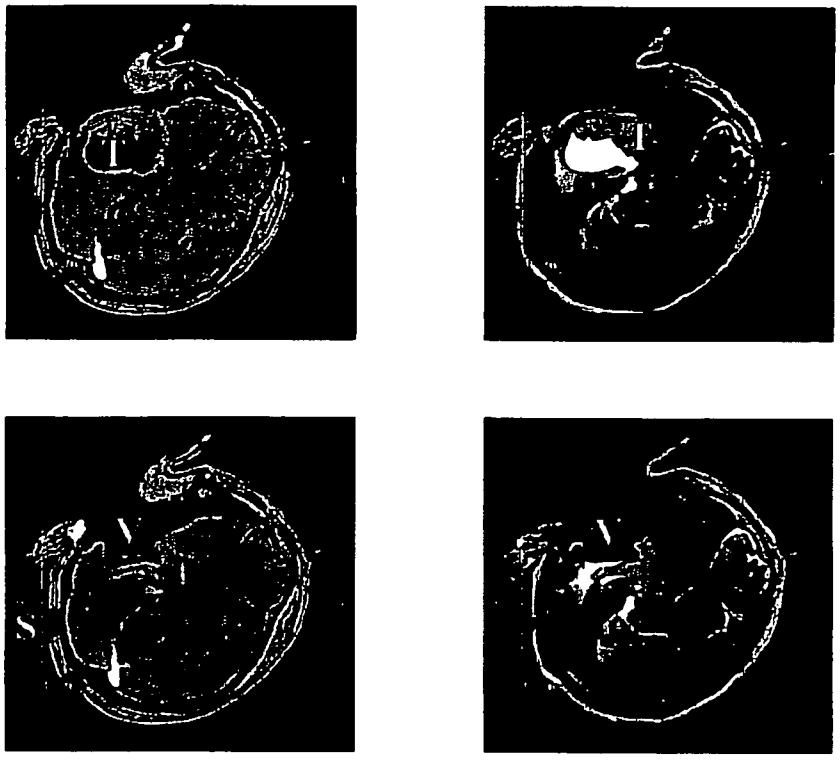

Figure 2

Axial intraoperative contrast-enhanced T_1-weighted (*left column*) and T_2-weighted (*right column*) images before (*upper row*) and after (*lower row*) removal of the temporal lobe glioblastoma, which were acquired with intraoperative MR scanner of low magnetic field strength (0.3 Tesla) using originally designed radiofrequency receiver coil integrated with modified Sugita head holder (headholder-coil). Note good image resolution, which permits their use for intraoperative neuronavigation, and minimal area of signal loss (S) at the point of contact of the titanium fixation pin with the scalp and cranium. Marked: tumor (T), resection cavity (V).

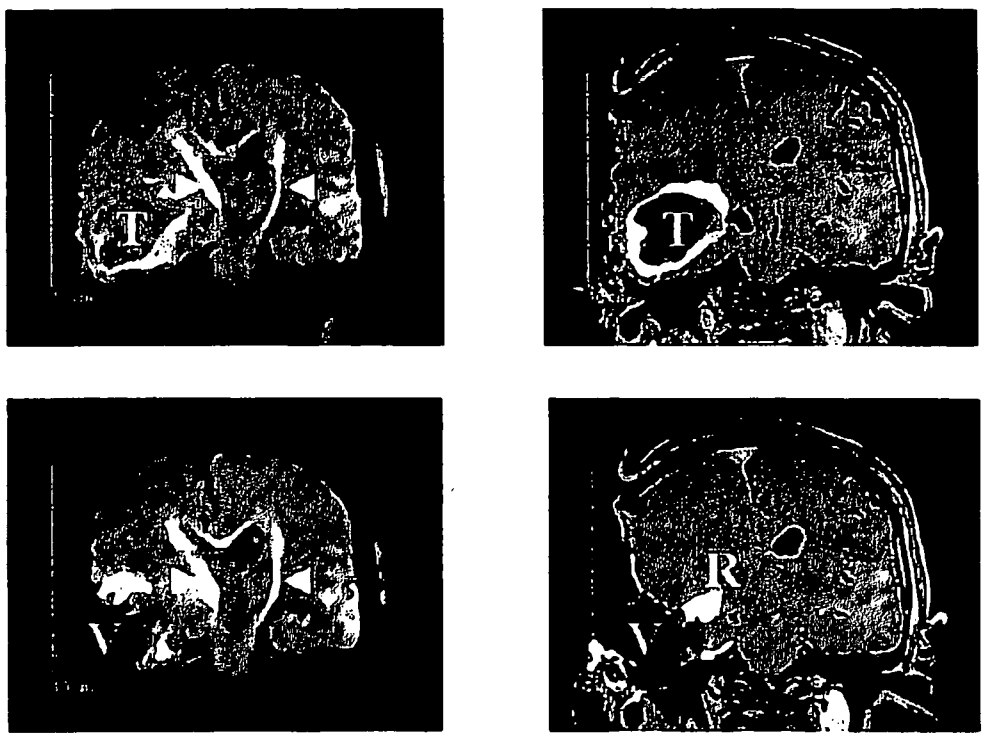

Figure 3

Coronal intraoperative diffusion-weighted (*left column*) and contrast-enhanced T_1-weighted (*right column*) images before (*upper row*) and after (*lower row*) removal of the temporal lobe glioblastoma, which were acquired with intraoperative MR scanner of low magnetic field strength (0.3 Tesla) using originally designed radiofrequency receiver coil integrated with modified Sugita head holder (headholder-coil). Note good image resolution, which permits their use for intraoperative neuronavigation, and clear visualization of the pyramidal tract with diffusion-weighted imaging. Marked: tumor (T), resection cavity (V), residual part of the neoplasm after its incomplete resection (R).

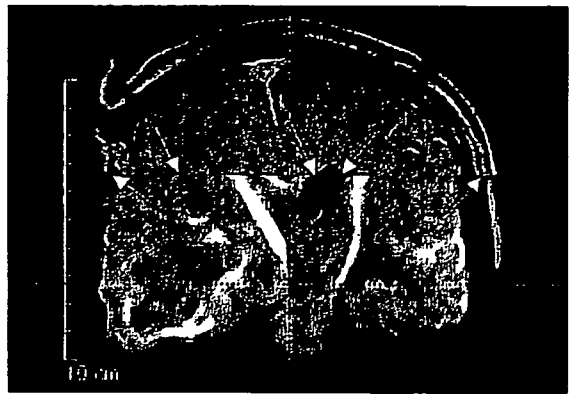

Figure 4

An intraoperative diffusion-weighted image with insufficient visualization of the pyramidal tract on the affected side compared to the non-affected side (*arrowheads*). Marked: peritumoral edema (E).

Figure 5

Evaluation of accuracy of the intraoperative DWI (*lower part*) superimposed on corresponding T_1-weighted image (*upper part*). Note that, with exception of cortical surface, there was good correspondence of the anatomical landmarks localization (*arrows*).

Sentinel node navigation segmentectomy for clinical stage IA non–small cell lung cancer

Hiroaki Nomori, MD, PhD,[a] Koei Ikeda, MD, PhD,[a] Takeshi Mori, MD,[a] Hironori Kobayashi, MD,[a] Kazunori Iwatani, MD,[a] Koichi Kawanaka, MD, PhD,[b] Shinya Shiraishi, MD, PhD,[b] and Toshiaki Kobayashi, MD, PhD[c]

From right to left: Drs Nomori, Mori, and Ikeda. The Bronze statue is Dr Shibasaburo Kitasato

Objective: Intraoperative frozen section examination of sentinel lymph nodes was conducted to determine the final indication for segmentectomy for clinical T1 N0 M0 non–small cell lung cancer.

Methods: Between April 2005 and July 2006, 52 patients with clinical T1 N0 M0 non–small cell lung cancer were prospectively treated by segmentectomy with sentinel node identification. The day before surgery, technetium-99m tin colloid was injected into the peritumoral region. After segmentectomy and lymph node dissection, sentinel nodes identified by measuring radioactive tracer uptake were examined for intraoperative frozen sections, which were serially cut 2 to 3 mm in thickness. When sentinel node metastasis was observed, segmentectomy was converted to lobectomy.

Results: Sentinel nodes were identified in 43 (83%) patients. The average number of sentinel nodes was 1.6 ± 0.9 (range: 1–5) per patient. Of 3 patients with metastatic sentinel lymph nodes, 2 underwent lobectomy and 1 larger segmentectomy. None of the other 40 patients had metastatic sentinel lymph nodes and therefore they were treated with segmentectomy. Pathologic staging with permanent sections was N0 in all of the 40 patients. On the other hand, in 9 patients whose sentinel nodes could not be identified, intraoperative frozen sections were required for 5.4 ± 2.3 lymph nodes, which was significantly more than 1.6 ± 0.9 in the 43 patients with sentinel node identification ($P < .001$).

Conclusion: Sentinel node identification is useful to determine the final indication of segmentectomy for clinical T1 N0 M0 non–small cell lung cancer by targeting the lymph nodes needed for intraoperative frozen section diagnosis.

From the Departments of Thoracic Surgery[a] and Radiology,[b] Graduate School of Medical Sciences, Kumamoto University, Honjo, Kumamoto, Japan; and the Department of Assistive Diagnostic Technology,[c] National Cancer Center Hospital, Tokyo, Japan.

This work was supported, in part, by Grant-in-Aid from the Ministry of Health, Labor, and Welfare, Japan.

Received for publication Aug 20, 2006; revisions received Oct 7, 2006; accepted for publication Oct 23, 2006.

Address for reprints: Hiroaki Nomori, MD, PhD, Department of Thoracic Surgery, Graduate School of Medical Sciences, Kumamoto University, 1-1-1 Honjo, Kumamoto 860-8556, Japan (E-mail: hnomori@qk9.so-net.ne.jp).

J Thorac Cardiovasc Surg 2007;133:780-5

0022-5223/$32.00

doi:10.1016/j.jtcvs.2006.10.027

GTS

In 1995, the Lung Cancer Study Group[1] conducted a prospective randomized controlled trial of limited resection versus lobectomy for clinical T1 N0 M0 non–small cell lung cancer (NSCLC) and concluded that the former was inferior to the latter regarding local recurrence and survival. However, the limited resection group in the study included both segmentectomy and wedge resection, and the curability for T1 N0 M0 NSCLC differed between the two procedures. On the other hand, there have been several reports describing that survivals were similar between patients treated with segmentectomy and those with lobectomy.[2-7]

The most important issue regarding segmentectomy versus lobectomy is whether postoperative local recurrence is increased. Whereas Warren and Faber[8] reported local recurrence in 15 (22.7%) of 66 patients after segmentectomy versus 5 (4.9%) of 103 patients after lobectomy, other authors reported that local recurrence after segmentectomy with complete dissection of hilar and mediastinal lymph nodes was equal to that after lobectomy.[3-6] However, for determining the final indication for segmentectomy, intraoperative frozen sections must be examined for all of the hilar

Abbreviations and Acronyms

CT = computed tomography
FDG-PET = fluorodeoxyglucose–positron emission tomography
NSCLC = non–small cell lung cancer
SN = sentinel node
SPECT = single photon emission computed tomography

and lobe-specific mediastinal lymph nodes to confirm the intraoperative N staging to be N0.[3-6]

A sentinel node (SN) is defined as the first lymph node within the lymphatic basin reached by lymph draining from the primary lesion. Recently, SNs have been identified by a radioactive tracer with or without dye during surgery for melanoma, breast cancer, gastrointestinal cancer, and lung cancer to reduce lymph node dissection.[9-14] We[13,14] previously reported that SN identification with technetium-99m tin colloid could establish the first site of nodal metastasis in NSCLC.

In the present study, we used SN identification to target the lymph nodes submitted for intraoperative frozen section diagnosis, which might determine the indication of segmentectomy. In addition, unlike Tsubota,[3] Okada,[4] Yoshikawa,[5] and their associates, who proposed that the indication for segmentectomy was T1 N0 M0 NSCLC less than 2 cm in size, we proposed that it was T1 N0 M0 NSCLC without size limitation. Because SN identification served as the final indication of segmentectomy, we named the procedure "sentinel node navigation segmentectomy."

Patients and Methods

Eligibility

The study protocol for SN navigation segmentectomy was approved by the Ethics Committee of Kumamoto University Hospital in March 2005. Informed consent was obtained from all patients after discussing the risks and benefits of the proposed surgery with their surgeons.

Patients

Between April 2005 and July 2006, 103 patients with NSCLC underwent surgical treatment. Of these, 73 patients had stage c-T1 N0 M0 cancer according to the findings of both computed tomography (CT) and fluorodeoxyglucose–positron emission tomography (FDG-PET). SN navigation segmentectomy was prospectively performed when (1) c-T1 N0 M0 NSCLC was identified in the peripheral lung; (2) the tumor on CT was more than 2 cm away from the pulmonary vein running at the boundary of the affected segment; (3) intraoperative frozen sections of SN showed no metastasis; (4) the surgical margin was intraoperatively found to be more than 2 cm from the tumor; and (5) tumors located centrally within the inner one third of the lung or in the right middle lobe were excluded. The stage of disease was based on the TNM classification of the International Union Against Cancer.[15] The lymph node nomenclature used was according to the lymph node map of Naruke and associates,[16] which was approved by the Japan Lung Cancer Society (Table 1).

TABLE 1. Lymph node nomenclature

N2 node	N1 node
Superior mediastinal	Hilar
No. 1. Highest mediastinal	No. 10. Hilar
No. 2. Paratracheal	No. 11. Interlobar
No. 3. Pretracheal	No. 12. Lobar
No. 4. Tracheobronchial	
Aortic	Intrapulmonary
No. 5. Botallo	No. 13. Segmental
No. 6. Para-aortic	No. 14. Subsegmental
Inferior mediastinal	
No. 7. Subcarinal	
No. 8. Paraesophageal	
No. 9. Pulmonary ligament	

Administration of Radioactive Colloid

The day before surgery, a 23-gauge needle was introduced into the peritumoral region under single photon emission computed tomography/computed tomography (SPECT/CT) system guidance, which incorporates a gantry-free SPECT with dual-head detectors (Skylight; ADAC Laboratories, Milpitas, Calif) and an 8 multidetector CT scanner (Light-Speed Ultra; General Electrics, Milwaukee, Wis). Technetium tin colloid (6–8 mCi) suspended in a 1- to 1.5-mL volume was injected in a single shot. SPECT/CT was performed 5 minutes after the injection and the next morning just before the operation.

SN Identification

The radioactivity of the resected lymph nodes was counted with a handheld gamma probe (Navigator; Auto Suture Japan, Tokyo, Japan). The radioactivity was measured for a 10-second period. SN was defined as any node for which the count was more than 5 times the radioactivity of the resected tissue with the lowest count.

SN Navigation Segmentectomy

Under thoracotomy, SN navigation segmentectomy was performed as follows: (1) Pulmonary arteries and bronchi of the affected segments were cut at the hilum; (2) pulmonary veins along the boundary of segments were isolated from the center to periphery; (3) the affected segments along the pulmonary veins were resected with staplers; (4) the hilar and systematic mediastinal lymph nodes were dissected; (5) the radioactivity of dissected lymph nodes was counted for SN identification; (6) SNs were examined by intraoperative frozen sections, which were serially cut 2 to 3 mm in thickness; (7) if the intraoperative frozen sections of the SN showed no metastasis, the operation was completed with segmentectomy; (8) if the sections of the SN showed metastasis, lobectomy was performed; and (9) if the SN could not be identified because radioactivity of the lymph nodes was low, all of the hilar and lobe-specific mediastinal lymph nodes were submitted for

GTS

TABLE 2. Sites of segmentectomy

Segment	No. of patients	Segment	No. of patients
Right		Left	
Upper lobe		Upper lobe	
S1	3	S1 + 2	4
S2	2	S3	2
S1 + S2	2	S1 + 2 + 3	9
S3	2	S4 + 5	7
S3 + S2b	1		
S2 + S3a	1		
Lower lobe		Lower lobe	
S6	4	S6	3
S7 + 8	1	S8	1
S8	1	S8 + 9	2
S9 + S10	2	S9 + 10	1
S7–10	1	S10	1
S6 + S9 + S10	1	S8–10	1
Total	21		31

Right upper lobe: *S1*, apical; *S2*, anterior; *S3*, posterior. Right lower lobe: *S6*, apical; *S7*, medial; *S8*, anterior; *S9*, lateral; *S10*, posterior. Left upper lobe: *S1+2*, apical posterior; *S3*, apical anterior; *S4*, superior lingular; *S5*, inferior lingular. Left lower lobe: *S6*, apical; *S8*, anterior; *S9*, lateral; *S10*, posterior.

TABLE 3. Characteristics of patients with and without sentinel node identification

	Sentinel lymph node	
	Identifiable	Nonidentifiable
Mean age (y)	69 ± 7	71 ± 7
Sex		
Male	26	8
Female	17	1
Mean tumor size (cm)	1.9 ± 0.7	2.1 ± 0.7
Histologic type		
Adenocarcinoma	37	6
Squamous cell carcinoma	4	2
Adenosquamous carcinoma	2	1
No. of lymph nodes submitted for intraoperative frozen diagnosis	1.6 ± 0.9	5.4 ± 2.3*
Pathologic TNM		
T1 N0 M0	39	9
T2 N0 M0	1	0
T1 N1 M0	1	0
T2 N1 M0	1	0
T1 N2 M0	1	0
Total	43	9

*$P < .001$.

intraoperative frozen section. Lobe-specific lymph nodes were defined as follows: No. 3 and No. 4 for the right upper lobe, No. 5 for the left upper lobe, and No. 7 for the lower lobe of both sides.[17]

Primary End Points of the Study

Primary end points of the study are as follows: (1) Can SN identification diagnose pathologic N stage during segmentectomy? (2) Are the survival and local recurrence after SN navigation segmentectomy similar to those after lobectomy?

Statistical Analysis

All data were analyzed for significance by the 2-tailed Student *t* tests. All values in the text and tables are given as mean ± SD.

Results

Operative procedures for the 73 patients with c-T1 N0 M0 were lobectomy in 12 patients, segmentectomy in 52, and wedge resection in 9. The reasons for conducting lobectomy in the 12 patients were as follows: (1) tumors in the right middle lobe in 5 patients; (2) tumors located centrally in 5 patients; (3) multiple lesions in the same lobe in 1 patient; and (4) thoracoscopic lobectomy as requested by the patient. As a result, 52 patients were consecutively enrolled for SN navigation segmentectomy. Table 2 shows the sites of segmentectomy for the 52 patients. The average number of dissected lymph node stations and lymph nodes per patient was 6 ± 1.8 stations and 12.5 ± 5.9 lymph nodes, respectively. Among the 52 patients, SNs could be identified in 43 (83%). The time needed for SN identification was within 5 minutes in each patient. The characteristics of the 43 patients with SN identification and of the 9 patients without are shown in Table 3. Average tumor size on CT was 1.9 ± 0.7 cm (range: 0.8–3.0 cm) and 2.1 ± 0.7 cm (range: 1.4–3.0 cm) in the patients with and without SN identification, respectively. Seventeen (40%) of the 43 patients with SN identification and 4 (44%) of 9 patients without had tumors larger than 2 cm. Pathologic tumor stages in the 43 patients with SN identification were T1 N0 M0 in 39, T2 N0 M0 in 1, T1 N1 M0 in 1, T2 N1 M0 in 1, and T1 N2 M0 in 1, whereas the stage in all 9 patients without SN identification was p-T1 N0 M0. The tumors in 2 patients were pathologically classified as T2; one tumor was spread over the pleura and the other was more than 3 cm in size in the permanent section. The average number of lymph nodes submitted for intraoperative frozen section examination was significantly less in the 43 patients with SN identification (1.6 ± 0.9 [range: 1–5] per patient) than in the 9 patients without SN identification (5.4 ± 2.3 [range: 3–10] per patient) ($P < .001$).

Table 4 shows the SN identified in the hilar lymph node stations. The number of stations having SN increased in numeric order from No. 10 to 13 stations. In the mediastinal lymph node stations, the SN was identified in 15 of the 43 patients (35%). Eleven of the 15 patients had SNs in both the hilar and mediastinal lymph node stations, whereas the remaining 4 patients had SNs only in the mediastinum. The distribution of mediastinal SNs is shown in Table 5, which